

Numerical studies of stabilized Townes solitons

Gaspar D. Montesinos and Víctor M. Pérez-García

*Departamento de Matemáticas, E.T.S.I. Industriales,
Universidad de Castilla-La Mancha, Ciudad Real, 13071 Spain.*

Abstract

We study numerically stabilized solutions of the two-dimensional Schrödinger equation with a cubic nonlinearity. We discuss in detail the numerical scheme used and explain why choosing the right numerical strategy is very important to avoid misleading results. We show that stabilized solutions are Townes solitons, a fact which had only been conjectured previously. Also we make a systematic study of the parameter regions in which these structures exist.

Key words: Nonlinear waves, Bose-Einstein condensation, blow-up phenomena

1 Introduction

In this paper we study systems ruled by the two-dimensional nonlinear Schrödinger equation (NLSE) [1,2] with a cubic time-dependent nonlinearity. More precisely we look for solutions of the Cauchy problem

$$i\frac{\partial u}{\partial t} = \left[-\frac{1}{2}\Delta + g(t)|u|^2 \right] u \quad (1a)$$

$$u(x, 0) = u_0(x) \in H^1(\mathbb{R}^2) \quad (1b)$$

where $u(x, t) : \mathbb{R}^2 \times \mathbb{R}^+ \rightarrow \mathbb{C}$, $\Delta = \partial^2/\partial x_1^2 + \partial^2/\partial x_2^2$ and $g(t)$ is a real function (the nonlinear coefficient) so that if $g < 0$ the nonlinearity is attractive whereas for $g > 0$ the nonlinearity is repulsive.

When g is a real constant Eq. (1a) is the cubic NLSE, which is one of the most important models of mathematical physics, with applications in very different fields [1,2].

It is well known that for $g < 0$ if $N \equiv \|u_0\|_2^2$, is above a threshold value N_c , solutions of Eq. (1a) can self-focus and become singular in a finite time. This phenomenon is called *wave collapse* or *blowup of the wave amplitude*. More precisely, there is no blowup when $N < N_c$ but for any $\epsilon > 0$, there exist solutions with $N = N_c + \epsilon$ for which there is blowup [3,4].

Eq. (1a) admits stationary solutions of the form $u(x, t) = e^{i\mu t}\Phi_\mu(x)$, where $\Phi_\mu(x)$ verifies

$$\Delta\Phi_\mu - 2\mu\Phi_\mu - 2g|\Phi_\mu|^2\Phi_\mu = 0. \quad (2)$$

As it is precisely stated in [1], when g is negative, for each positive μ there exists only one solution of Eq. (2) which is real, positive and radially symmetric and for which $\int |\Phi_\mu|^2 d^2x$ has the minimum value between all of the possible solutions of Eq. (2). Moreover, the positivity of μ ensures that this solution decays exponentially at infinity. This solution is called the *ground state* or *Townes soliton*. We will denote this solution as $R_\mu(r)$ which satisfies

$$\Delta R_\mu - 2\mu R_\mu - 2gR_\mu^3 = 0 \quad (3)$$

$$\lim_{r \rightarrow \infty} R_\mu(r) = 0, \quad R'_\mu(0) = 0. \quad (4)$$

Once the value of μ is fixed, the power and width of R_μ are given by $N_\mu = \int |R_\mu|^2 d^2x$ and $W_\mu = (\int |R_\mu|^2 r^2 d^2x)^{1/2}$ respectively. By applying scaling transformations to $R_\mu(r)$ it is possible to build a family of Townes solitons having the same shape and norm but different widths

$$R_\mu(r) = \mu^{1/2} R_1(\mu^{1/2} r), \quad W_\mu = W_1 / \mu^{1/2}. \quad (5)$$

The equation which verifies the normalized soliton $R_{\mu,N}(r) = R_\mu(r)/N_\mu^{1/2}$ is

$$\Delta R_{\mu,N} - 2\mu R_{\mu,N} - 2gN_\mu R_{\mu,N}^3 = 0. \quad (6)$$

From the theory of nonlinear Schrödinger equations it is known that the Townes soliton has exactly the critical power for blowup N_c , therefore, it separates in some sense the region of collapsing and expanding solutions. Moreover, the Townes soliton is *unstable*, i.e. small perturbations of this solution lead to either expansion of the initial data or blowup in finite time.

The case where g is not constant but a continuous periodic function of t has arisen recently in different fields of applications of Eq. (1a). The intuitive idea is that (oscillating) bound states could be obtained by combining cycles of positive and negative g values so that after an expansion and contraction regime the solution could come back to the initial state. In this way some sort of pulsating trapped solution, i.e., a *breather*, could be generated.

This idea was first proposed in the field of nonlinear Optics [5]. In that context, two-dimensional solitary waves have been proposed for optical systems

[5,6,7]. There, a spatial modulation of the Kerr coefficient (the nonlinearity) of the optical material is used to prevent collapse so that the beam becomes collapsing and expanding in alternating regions and is stabilized in average. The same idea has been used in the field of matter waves in Refs. [8,9]. In Ref. [10] some general results are provided for generic nonlinearities. Finally in Ref. [11] stabilized vector solitons have been proposed and studied.

The aim of this paper is to study in more detail the stabilization mechanism. This paper is organized as follows: First, in Sec. 2 we present the numerical method used to integrate the equations, which involves a Fourier pseudospectral scheme, a split-step scheme and the use of an absorbing potential which allows to get rid of the radiation. In Sec. 3 we discuss the phenomenon of stabilization of solutions of the NLSE and show quantitatively that the structure that remains stabilized is a Townes soliton, thus confirming the conjecture raised in Ref. [10]. We also study the robustness of the stabilized soliton under parameter variations. Finally, in Sec. 4 we summarize our conclusions.

2 Numerical methods

2.1 Fourier pseudospectral scheme

In this paper we study Eq. (1a) numerically. To this end we have developed a Fourier pseudospectral scheme for the discretization of the spatial derivatives combined with a split-step scheme to compute the time evolution. Split-step schemes are based on the observation that many problems may be decomposed into exactly solvable parts and on the fact that the full problem may be approximated as a composition of the individual problems. For instance, the solution of partial differential equations of the type $\partial_t u(x, t) = N(t, x, u, \partial_x, \dots)u = (A + B)u$ can be approximated from the exact solutions of the problems $\partial_t u = Au$, and $\partial_t u = Bu$.

To approximate properly the solutions of Eq. (1a) we include an absorbing potential in the border of the simulation region to extract the outgoing radiation and provide some sort of local transparent boundary conditions. This potential may be included in Eq. (1a) as a complex term [12,13] so that the new equation we will discretize is

$$i\frac{\partial U}{\partial t} = \left[-\frac{1}{2}\Delta + g(t)|U|^2 - iV_a \right] U, \quad (7)$$

where $V_a(x)$ is a positive real function which must be chosen to maximize the absorption of the radiation while minimizing the effect on trapped structures (i.e. to mimic the behavior of true transparent boundary conditions). More-

over, $U(x, t) \simeq u(x, t)$ will satisfy specific boundary conditions on the border of the simulation region Ω_h . As $\Omega_h \rightarrow \mathbb{R}^2$ and $V_a \rightarrow 0$ we expect $U \rightarrow u$.

Let us decompose the evolution operator in Eq. (7) by taking [14,15]

$$A = \frac{i}{2}\Delta, \quad (8a)$$

$$B = -ig(t)|U|^2 - V_a. \quad (8b)$$

To proceed with split-step type methods it is necessary to compute the explicit form of the operators $e^{(t-t_0)A}$ and $e^{(t-t_0)B}$. To get the action of the operators we solve the subproblems

$$\partial_t U = \frac{i}{2}\Delta U, \quad (9a)$$

$$\partial_t U = -ig(t)|U|^2 U - V_a U. \quad (9b)$$

Since $U \in H^1(\mathbb{R}^2)$, Eq. (9a) can be solved in Fourier space. Denoting the spatial Fourier transform of U by $\hat{U}(k, t) = \mathcal{F}(U(x, t))$ we get

$$\partial_t \hat{U} = -\frac{i}{2}k^2 \hat{U}, \quad (10)$$

whose explicit solution is $\hat{U}(k, t) = \hat{U}(k, t_0)e^{-ik^2(t-t_0)/2}$.

To solve (9b) we write $U = \rho^{1/2}e^{i\phi}$ and substituting in Eq. (9b) we get, from the real part, $\dot{\rho} = -2V_a\rho$ whose solution is

$$\rho(t) = e^{-2V_a(t-t_0)}\rho(t_0). \quad (11)$$

The imaginary part of Eq. (9b) is $\dot{\phi} = -g(t)\rho$ whose solution is $\phi(t) = \phi(t_0) - \rho(t_0) \int_{t_0}^t g(s)e^{-2V_a(s-t_0)}ds$. Finally, we can write

$$U(t) = U(t_0) \exp\left(-V_a(t-t_0) - i\rho(t_0) \int_{t_0}^t g(s)e^{-2V_a(s-t_0)}ds\right). \quad (12)$$

In this way, by defining the time step τ as $\tau = (t-t_0)/c$, $c \in \mathbb{R}$, after a suitable renaming we obtain the explicit form of the operators

$$e^{(t-t_0)A} \equiv e^{c\tau A} = \mathcal{F}^{-1} \exp(-ic\tau k^2/2) \mathcal{F}, \quad (13a)$$

$$e^{(t-t_0)B} \equiv e^{c\tau B} = \exp\left(-V_a c\tau - i\rho(t) \int_t^{t+c\tau} g(s)e^{-2V_a(s-t)}ds\right). \quad (13b)$$

Specifically, when $g(t)$ is given by $g(t) = g_0 + g_1 \cos(\Omega t)$, as we have used in

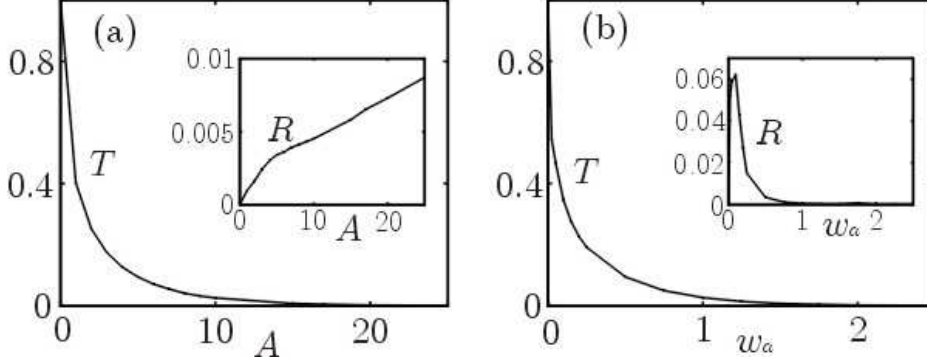


Fig. 1. Reflection (R) and transmission (T) coefficients (see text) for the collision of a Townes soliton with an absorbing potential $V_a = Ae^{-(r-r_0)^2/2w_a^2}$. (a) T and R as a function of A for $w_a = 0.5$. (b) T and R as a function of w_a for $A = 5$.

our simulations it is possible to write explicitly the integral in (13b) obtaining

$$-\int_t^{t+c\tau} g(s)e^{-2V_a(s-t)}ds = \frac{g_0}{2V_a} (e^{-2V_ac\tau} - 1) - \frac{g_1}{\Omega^2 + (2V_a)^2} \times \\ \times \left\{ e^{-2V_ac\tau} [\Omega \sin \Omega(t + c\tau) - 2V_a \cos \Omega(t + c\tau)] - (\Omega \sin \Omega t - 2V_a \cos \Omega t) \right\}.$$

Having the explicit form of the solutions of the subproblems (9) allows us to obtain the solution of Eq. (7) to any degree of accuracy. We have used two different splittings: the classical method of second order and a fourth order optimized method [16] whose equations are

$$U(x, t + \tau) = e^{\tau A/2} e^{\tau B} e^{\tau A/2} U(x, t) + \mathcal{O}(\tau^3), \quad (14a)$$

$$U(x, t + \tau) = e^{a_1 \tau A} e^{b_1 \tau B} e^{a_2 \tau A} e^{b_2 \tau B} e^{a_3 \tau A} e^{b_3 \tau B} e^{a_4 \tau A} e^{b_3 \tau B} e^{a_3 \tau A} \times \\ \times e^{b_2 \tau B} e^{a_2 \tau A} e^{b_1 \tau B} e^{a_1 \tau A} U(x, t) + \mathcal{O}(\tau^5). \quad (14b)$$

with $a_1 = 0.0829844064174052$, $b_1 = 0.245298957184271$, $a_2 = 0.396309801498368$, $b_2 = 0.604872665711080$, $a_3 = -0.0390563049223486$, $b_3 = 1/2 - (b_1 + b_2)$, $a_4 = 1 - 2(a_1 + a_2 + a_3)$. Both methods are symmetric compositions of operators. However, method (14a) requires only one evaluation of e^A and e^B (instead of two) per step because it is possible to concatenate terms using the First Same As Last (FSAL) property. For method (14b) the computational cost per step is much higher since even using the FSAL property the number of evaluations of e^A and e^B is six.

These schemes have many advantages. From the practical point of view the calculation of the Fourier transform, which is the most computer time-consuming step in the calculations, may be done by using the fast Fourier transform (FFT). Thus the computational cost of the method is of order $\mathcal{O}(\mathcal{N}^2 \log \mathcal{N})$, being \mathcal{N} the points number in each spatial direction of the grid which is quite acceptable. The use of discrete transforms to represent the continuous

Fourier transform in (14) implicitly imposes periodic boundary conditions on U . However, since U is expected to be negligible on the boundaries (otherwise the computational domain must be enlarged or the absorbing potential corrected) this is not an essential point. Another convenient property of these schemes is their preservation of the L^2 -norm of the solutions.

2.2 The absorbing potential

The implementation of transparent boundary conditions is essential to avoid misleading results as it will be clear later. This is because of the decomposition of initial data into trapped states plus some outgoing radiation, a situation which is typical of NLS problems with fixed coefficients [17,18] and also happens in the case at hand.

Specifically, we have chosen as absorbing potential $V_a = Ae^{-(r-r_0)^2/2w_a^2}$, where A, r_0 and w_a characterize the absorber. The choice of the parameter values must be done to maximize the absorption of the outgoing radiation. To choose optimal values we have made several tests by making a Townes soliton collides with absorbing potentials of several amplitudes and widths. We have computed the reflection (R) and transmission (T) coefficients defined as $R = |u_b|/|u_0|$, $T = |u_f|/|u_0|$ where u_0 , u_b and u_f are the initial data, the part of the initial data which moves backwards after reflection, and the part of the initial data which moves forward after crossing the absorbing potential, respectively.

Typical examples of the results are shown in Fig. 1. One must choose a value for A large enough to ensure a good absorption, whereas the width w_a of the absorbing potential cannot be chosen too large, since then either the effect on stabilized structures could be non-negligible or the integration region should be enlarged to non-practical sizes.

When the absorbing potential is absent the numerical simulations are misleading and the trapping effects are altered, because the radiation interacts with the stabilized structure leading to spurious destabilization. In Figs. 2 and 3 we illustrate this behavior starting with a Townes soliton as initial data.

3 Stabilization of solitons

3.1 What is the shape of stabilized solitons?

In Refs. [5,6,7,8,9,10] it has been shown that if g is an adequate periodic function $g(t)$ it is possible to obtain a stabilized structure starting from different

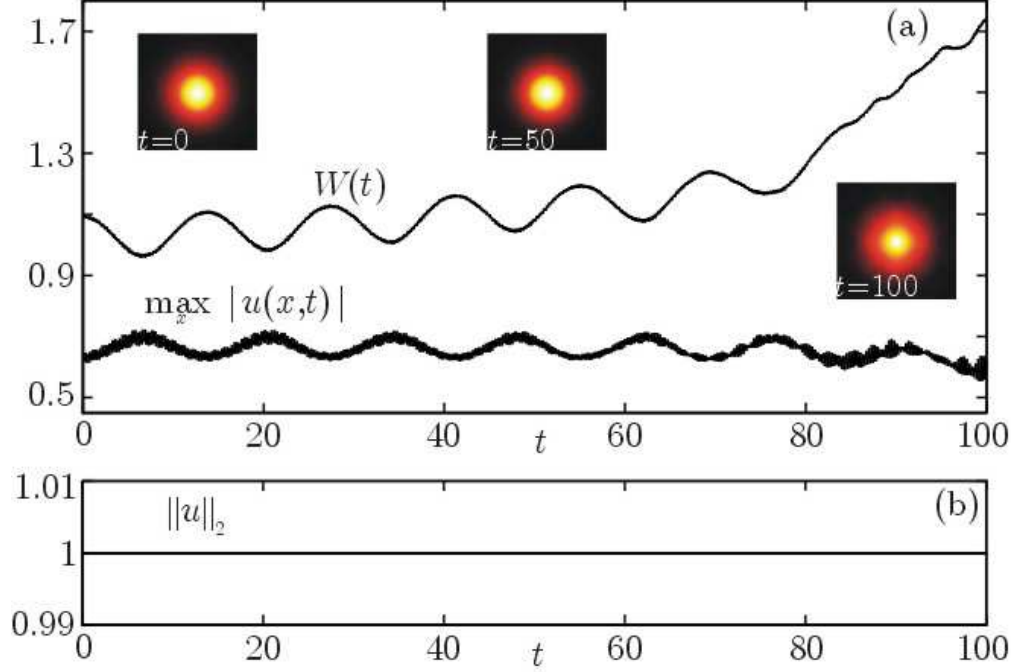


Fig. 2. Results of numerical simulations of Eq. (1a) showing evolution of the initial data $u(x,0) = R_{\mu,N}(x)$ with $\mu = 0.5$ and $g = -0.5$ ($W(0) = 1.09$) for parameter values $g_0 = -2\pi$, $g_1 = 8\pi$, $\Omega = 40$, *without absorbing potential*. (a) Evolution of the width $W(t)$ and of the amplitude $\max_x |u(x,t)|$. The insets show pseudo-color plots of $|u(x,t)|^2$ for different times. (b) Evolution of the norm $\|u\|_2$.

types of initial data, such as Townes solitons or Gaussian functions. In Figs. 3 and 4 we summarize results taking as initial data a Townes soliton and a Gaussian function, respectively.

In both cases we get stabilization but in the case of Gaussian initial data, a readjustment is produced by ejecting outside the central region a significant part of the wave packet. This happens during the first 10 time units where the width increases significantly due to the contribution of the outgoing wave. This wave is dissipated when hits the absorbing region leading to the step in the norm evolution shown in Fig. 4(b). It was also conjectured in Ref. [10] that the stabilized solution after this process might be a scaled Townes soliton (which would explain why the stabilization of the Townes soliton looks smoother). In this section we support this conjecture quantitatively with precise numerical simulations of Eq. (1a) using the numerical schemes of Sec. 2.

To study the shape of the stabilized soliton we define the error functional

$$E_\mu(t) = \frac{\| |u(x,t)| - |R_\mu(x)| \|_2}{\|u(x,t)\|_2}, \quad (15)$$

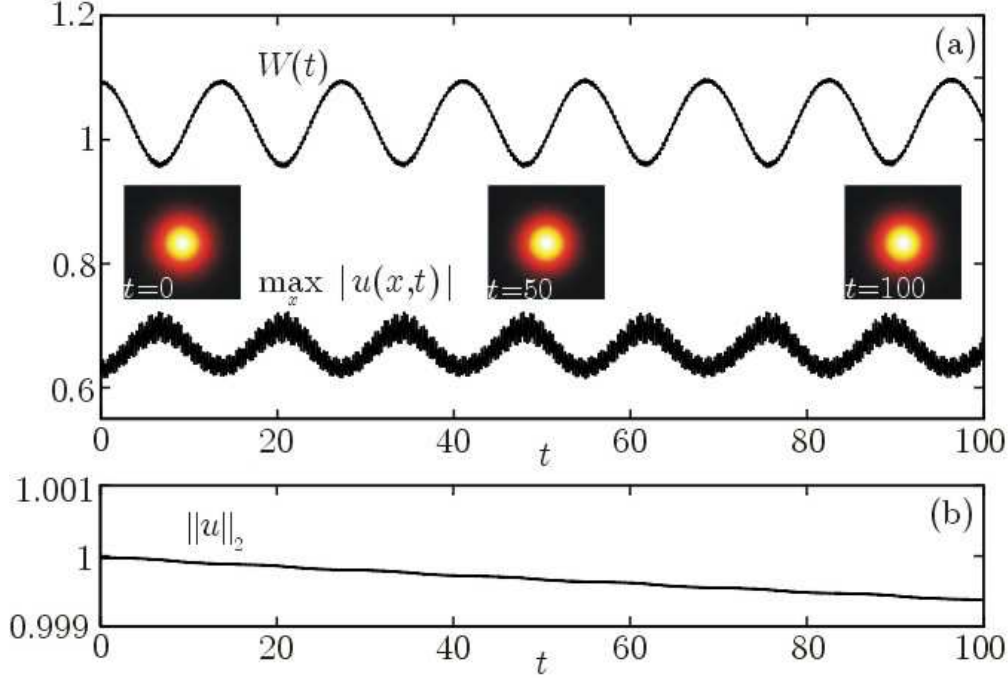


Fig. 3. Same as Fig. 2 but with absorbing potential.

and the error function $E(t)$ as $E(t) = \min_{\mu} E_{\mu}(t)$. Note that according to Eq. (5) the parameter μ parametrizes the shape of the Townes solitons in such a way that if μ increases the width of the soliton decreases and the amplitude increases. The error function $E(t)$ measures the distance between the solution of Eq. (1a) and the family of Townes solitons. We have computed numerically the function $E(t)$ by evaluating the integrals in (15) for a large set of μ values and then choosing the minimum between all of them.

In Fig. 5 we summarize our results when a Townes soliton is taken as initial data. We see, in Fig. 5(b) that E oscillates about a value of 0.02, with a maximum of about 0.03. This means that the solution of Eq. (1a) can be approximated by a Townes soliton at all times with a maximum error in the norm of about 3% which is definitely small. In fact, this number could be even compatible with zero taking into account the number of approximations involved in our computation: the discretization of Eq. (1a), the absorbing potential, the calculation of the integral (15) and the discrete set of μ values chosen to compute the minimum.

When Gaussian initial data are taken (Fig. 6) we start with an optimal fitting whose error is about 14%. This error decreases with time to a value around of 2% similar to the one in the Townes soliton case. This provides a quantitative support to the idea that Gaussian (or other) initial profiles evolve into a stabilized Townes soliton by ejecting a fraction of their amplitude in the form

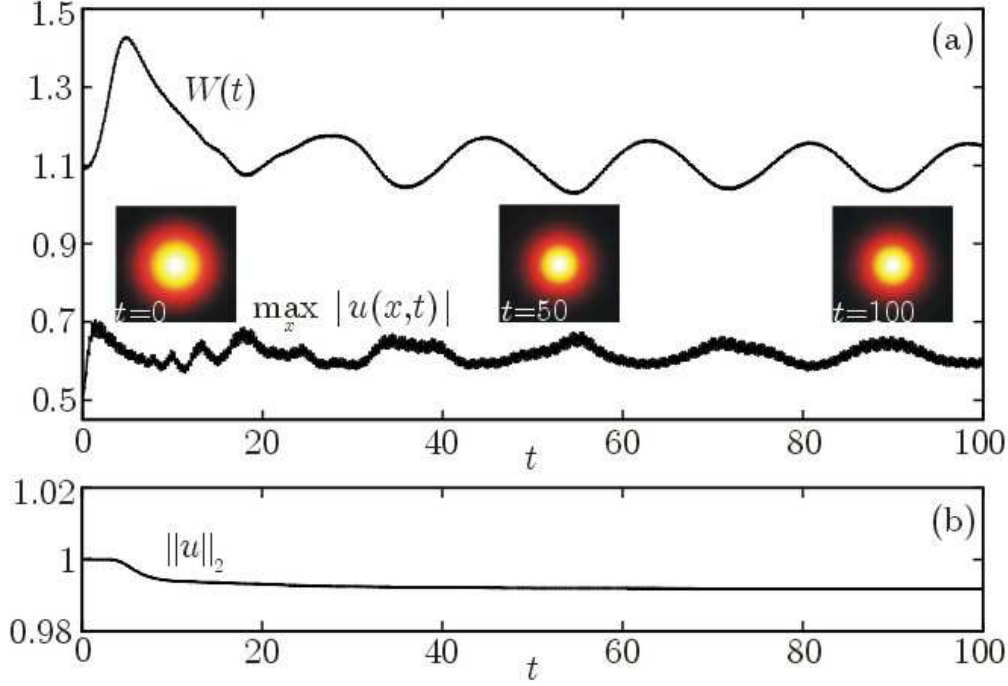


Fig. 4. Results of numerical simulations of Eq. (1a) showing stabilization of Gaussian initial data $u(x,0) = (1/\sqrt{\pi}w)e^{-r^2/2w^2}$ with $w = 1.09$ for parameter values $g_0 = -2\pi$, $g_1 = 8\pi$, $\Omega = 40$. (a) Evolution of the width $W(t)$ and of the amplitude $\max_x |u(x,t)|$. The insets show pseudocolor plots of $|u(x,t)|^2$ for different times. (b) Evolution of the norm $\|u\|_2$.

of radiation.

Moreover, in Figs. 5(a) and 6(a) we see that the minimum points μ_{min} evolve according to what we expected. They oscillate in phase opposition respect to the width evolution of the solutions (see Figs. 3 and 4), because an increase of the width corresponds to a decrease of μ and viceversa (see Eq. (5)).

3.2 Robustness of stabilized structures to parameter variations

Finally, to have an idea of the range of parameter values for which stabilization is possible, we have made simulations when a Townes soliton is taken as initial data moving the g_1 and Ω parameters ($g_0 = -2\pi$ fixed). We have found that for $\Omega \in [20, 250]$ and $g_1 \in [5\pi, 15\pi]$ the stabilization is possible although evolution of the width and of the amplitude shows different behaviors. In Fig. 7 we plot the results for several parameter values.

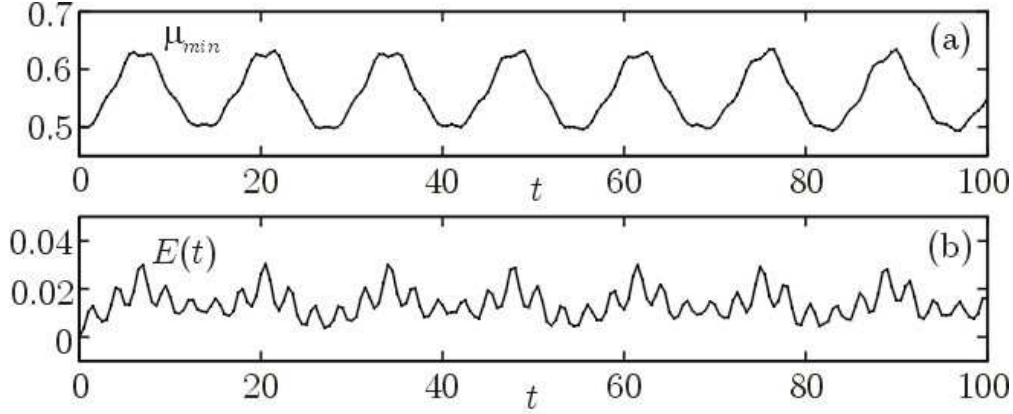


Fig. 5. Analysis of the solutions of Eq. (1a) for a Townes-soliton initial data. (a) Values of μ which minimize the error functional E_μ as a function of time. (b) Error function E as a function of time.

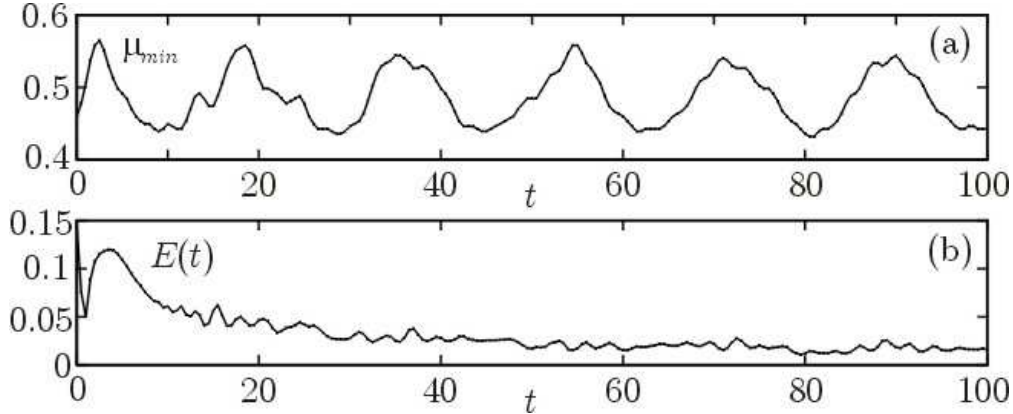


Fig. 6. Same as Fig. 5 but for Gaussian initial data.

4 Conclusions

In this paper we have developed an accurate numerical scheme to study the stabilization of solutions of the two-dimensional cubic nonlinear Schrödinger equation under variations of the nonlinear coefficient. We have also given numerical evidences in favor of the conjecture raised in Ref. [10] concerning the shape of stabilized solitons. Finally, we have shown that stabilization is possible in a wide range of parameter values which is an interesting result for the possible applications of these structures to the fields of Bose-Einstein condensation and nonlinear Optics.

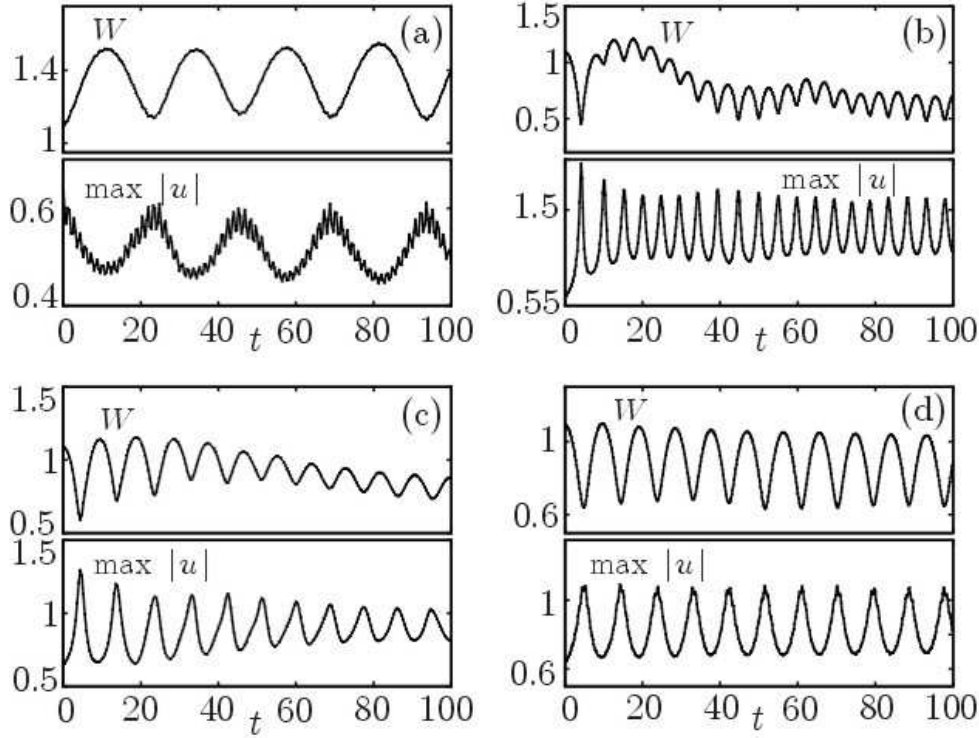


Fig. 7. Stabilization of $u(x, 0) = R_{\mu, N}(x)$ with $\mu = 0.5$ and $g = -0.5$ ($W(0) = 1.09$). Shown are the evolution of the width $W(t)$ and of the amplitude $\max_x |u(x, t)|$ for several parameter values. (a) $g_0 = -2\pi$, $g_1 = 6\pi$, $\Omega = 20$. (b) $g_0 = -2\pi$, $g_1 = 8\pi$, $\Omega = 250$. (c) $g_0 = -2\pi$, $g_1 = 6\pi$, $\Omega = 80$. (d) $g_0 = -2\pi$, $g_1 = 15\pi$, $\Omega = 150$.

Acknowledgements

This work has been supported by grants BFM2003-02832 (Ministerio de Ciencia y Tecnología) and PAC-02-002 (Consejería de Ciencia y Tecnología de la Junta de Comunidades de Castilla-La Mancha). G. D. M. is supported by Ministerio de Educación, Cultura y Deporte under grant AP2001-0535.

References

- [1] C. Sulem and P. Sulem, The nonlinear Schrödinger equation: Self-focusing and wave collapse, Springer, Berlin (2000).
- [2] L. Vázquez, L. Streit, V. M. Pérez-García, Eds., Nonlinear Klein-Gordon and Schrödinger systems: Theory and Applications, World Scientific, Singapore (1996).
- [3] G. Fibich and G. Papanicolaou, Self-focusing in the perturbed and unperturbed nonlinear Schrödinger equation in critical dimension, SIAM J. Appl. Math. **60**,

183-240 (1999).

- [4] M. I. Weinstein, Non-linear Schrödinger-equations and sharp interpolation estimates, *Commun. Math. Phys.* **87**, 567-576 (1983).
- [5] L. Berge, V. K. Mezentsev, J. J. Rasmussen, P. L. Christiansen and Y. B. Gaididei, Self-guiding light in layered nonlinear media, *Opt. Lett.* **25**, 1037-1039 (2000).
- [6] I. Towers and B. A. Malomed, Stable (2+1)-dimensional solitons in a layered medium with sign-alternating Kerr nonlinearity, *J. Opt. Soc. Am. B* **19**, 537-543 (2002).
- [7] A. Kaplan, B. V. Gisin, B. A. Malomed, Stable propagation and all-optical switching in planar waveguide-antiwaveguide periodic structures, *J. Opt. Soc. Am. B* **19**, 522-528 (2002).
- [8] H. Saito and M. Ueda, Dynamically stabilized bright solitons in a two-dimensional Bose-Einstein condensate, *Phys. Rev. Lett.* **90**, 040403 (2003).
- [9] F. Abdullaev, J. G. Caputo, R. A. Kraenkel, and B. A. Malomed, Controlling collapse in Bose-Einstein condensates by temporal modulation of the scattering length, *Phys. Rev. A* **67**, 013605 (2003).
- [10] G. D. Montesinos, V. M. Pérez-García, P. Torres, Stabilization of solitons of the multidimensional nonlinear Schrödinger equation: Matter-wave breathers, e-print arxiv.org/nlin.PS/0305030 (to appear in *Physica D*).
- [11] G. D. Montesinos, V. M. Pérez-García, H. Michinel, Stabilized two-dimensional vector solitons, e-print arxiv.org/nlin.PS/0310020.
- [12] P. Tran, Solving the time-dependent Schrödinger equation: Suppression of reflection from the grid boundary with a filtered split-operator approach, *Phys. Rev. E* **58**, 8049-8051 (1998).
- [13] T. Fevens, H. Jiang, Absorbing boundary conditions for the Schrödinger equation, *SIAM J. Sci. Comput.* **21**, 255-282 (1999).
- [14] T. R. Taha and M. J. Ablowitz, Analytical and numerical aspects of certain nonlinear evolution equations .2. Numerical, Nonlinear Schrödinger equation, *J. Comp. Phys.* **55** (1984) 203-230.
- [15] V. M. Pérez-García and X. Liu, Numerical methods for the simulation of trapped nonlinear Schrödinger systems, *Appl. Math. Comput.* **144**, 215-235 (2003).
- [16] S. Blanes and P. C. Moan, Practical symplectic partitioned Runge-Kutta and Runge-Kutta-Nystrom methods, *J. Comp. Appl. Math.* **142**, 313-330 (2002).
- [17] S. Cuccagna, Stabilization of Solutions to Nonlinear Schrödinger Equations, *Commun. Pure Appl. Math.* **54**, 1110-1145 (2001).
- [18] T. P. Tsai, H. T. Yau, Asymptotic dynamics of nonlinear Schrödinger equations: Resonance-dominated and dispersion-dominated solutions, *Comm. Pure Appl. Math.* **55**, 153-216 (2002).